

# Using conditional entropy to identify periodicity

Matthew J. Graham,<sup>★</sup> Andrew J. Drake, S. G. Djorgovski, Ashish A. Mahabal  
and Ciro Donalek

*California Institute of Technology, 1200 E. California Blvd, Pasadena, CA 91125, USA*

Accepted 2013 June 27. Received 2013 June 26; in original form 2013 June 4

## ABSTRACT

This paper presents a new period-finding method based on conditional entropy that is both efficient and accurate. We demonstrate its applicability on simulated and real data. We find that it has comparable performance to other information-based techniques with simulated data but is superior with real data, both for finding periods and for just identifying periodic behaviour. In particular, it is robust against common aliasing issues found with other period-finding algorithms.

**Key words:** methods: data analysis – techniques: photometric – astronomical data bases: miscellaneous.

## 1 INTRODUCTION

The growing amount of astronomical time series data provided by the new generation of synoptic sky surveys, e.g. Catalina Real-time Transient Survey (CRTS; Drake et al. 2009), Palomar Transient Factory (PTF; Rau et al. 2009), Pan-STARRS (Kaiser et al. 2002), LSST (Ivezic et al. 2011), has fostered a renewed interest in period-finding algorithms (e.g. Huijse et al. 2011, 2012; Kato & Uemura 2012; Leroy 2012; Baluev 2013). There is a particular emphasis on efficiency, both in terms of speed and accuracy, to facilitate tractable analyses of tera- and peta-scale data sets. Period-finding techniques can be divided into a number of types. The most popular seek to model a light curve via a least-squares fit to some set of (orthogonal) basis functions, most commonly trigonometric, such as Lomb–Scargle (Lomb 1976; Scargle 1982) and its derivatives/extensions (e.g. Zechmeister & Kurster 2009), though more complicated function sets, such as wavelets (Foster 1996), have also been tried. Another approach is to minimize some measure of the dispersion of time series data in phase space, such as binned means (Stellingwerf 1978), variance (Schwarzenberg-Czerny 1989) or entropy (Cincotta, Mendez & Nunez 1995), which can often be regarded as an expansion in terms of periodic orthogonal step functions. Bayesian methods (Gregory & Loredo 1992; Wang, Khardon & Protopapas 2012) are also becoming common and there have even been attempts to search for periodicity using neural networks (Baluev 2012).

The basis of an algorithm also often determines how well it copes with the real world aspects of time series data, such as irregular sampling, gaps and errors, e.g. standard Fourier analysis is impossible for any data diverging from regular sampling. de Jager, Raubenheimer & Swanepoel (1989) argue that in the case of weak signals,

most period-finding methods only work well with certain kinds of periodic shapes and that this causes a selection effect for the general identification of weak periodic signals. Similar shape dependences are found in Schwarzenberg-Czerny (1999).

Intuitively, the fastest period-finding algorithm will involve a single pass through a data set per trial period and integer counting operations, e.g. histogram binning. Any higher order function calls, particularly per data point in a time series, will extend the average calculation time per trial period and, consequently, the overall time taken by the algorithm to determine a correct period.

Among the different types of approaches – Fourier-based, Bayesian, autoregressive modelling, etc. – one of the most promising is information theory as this type of technique seems better equipped to deal with uneven sampled time series (as most modern light curves are). Information theory-based methods extract information from the probability density function and so include higher order statistical moments present in the data whereas Fourier or analysis of variance (AOV) techniques are based only on second-order statistical analyses. This implies that information theory brings better modelling of the underlying process and robustness to noise and outliers. Huijse et al. (2012) employ information theory-based statistical descriptors, such as Renyi quadratic entropy and correntropy, which are generalizations of second-order moment statistics such as variance and correlation.

Cincotta et al. (1995) introduced a method to find the period of an (irregularly sampled) time series by minimizing its Shannon entropy when folded by a trial period. The idea is that a light curve folded at most trial periods will produce a random arrangement of points in a particular region, a unit square, say, whereas, when folded at the correct period, the light curve will be the most ordered arrangement of data points in the region and so contain the most information about the signal. As entropy measures the lack of information about a system, the correct period minimizes this quantity. Moreover, this can be formally proven to be mathematically correct within the

<sup>★</sup>E-mail: mjpg@caltech.edu

framework of information theory (Cincotta et al. 1999) whilst other measures based on the statistical analysis of the ‘shape’ of the light curve lack a formal proof.

In this work, we introduce a new technique based on the *conditional* Shannon entropy of a light curve. This has the advantage of accounting for systematic effects in the phase space coverage of time series, i.e. gaps, concentrations and other artefacts that may be present in the phase distribution when the light curve is folded by a trial period as a result of sampling.

The paper is structured as follows: in Section 2, we present the new algorithm and in Section 3, the data sets we have applied it to. We discuss our results in Section 4 and conclusions in Section 5.

## 2 ALGORITHMS

### 2.1 Conditional entropy

Formally, a time series,  $m(t_i)$ , is normalized to occupy a unit square in the  $(\phi, m)$  plane where  $\phi_i$  is the phase at  $t_i$  given a trial period,  $p$ , such that  $\phi_i = t_i/p - [t_i/p]$ , where the square brackets denote the integer function. The unit square is then partitioned into  $k$  partitions (bins), and the (Shannon) entropy for the distribution,  $H_0$ , is defined by

$$H_0 = - \sum_{i=1}^k \mu_i \ln(\mu_i) \quad \forall \mu_i \neq 0, \quad (1)$$

where  $\mu_i$  is the occupation probability for the  $i$ th partition, which is just the number of data points in that partition divided by the total number of points in the data set.

However, on applying this method to real data, e.g. a typical type AB RR Lyrae from CRTS (Drake et al. 2013) (see Fig. 1), we found that the period which minimized the entropy was predominantly that associated with the mean solar day ( $p = 1.00274$  d). Looking at a folded light curve at this period (see Fig. 1b), it is clear that this does indeed produce the most ordered arrangement of points in terms of compactness of points within the unit square; however, this is not the most ordered in terms of an underlying functional support which the correct period would produce. Another way of expressing this is that with the solar period, the order of points per phase interval is not optimized whereas it is with the true period – the amount of randomness in the normalized magnitude is minimized given the known values of the phase. We note that this effect can be mitigated to some degree through an appropriate choice of partition (Cincotta 1999) but this then introduces an additional step into the period-finding process.

A related quantity taking this into account is the *conditional* entropy (CE),  $H(m|\phi)$ , defined by

$$H_c = \sum_{i,j} p(m_i, \phi_j) \ln \left( \frac{p(\phi_j)}{p(m_i, \phi_j)} \right), \quad (2)$$

where  $p(m_i, \phi_j)$  is the occupation probability for the  $i$ th partition in normalized magnitude and the  $j$ th partition in phase and  $p(\phi_j)$  is the occupation probability of the  $j$ th phase partition, which for rectangular partitions is just

$$p(\phi_j) = \sum_i p(m_i, \phi_j).$$

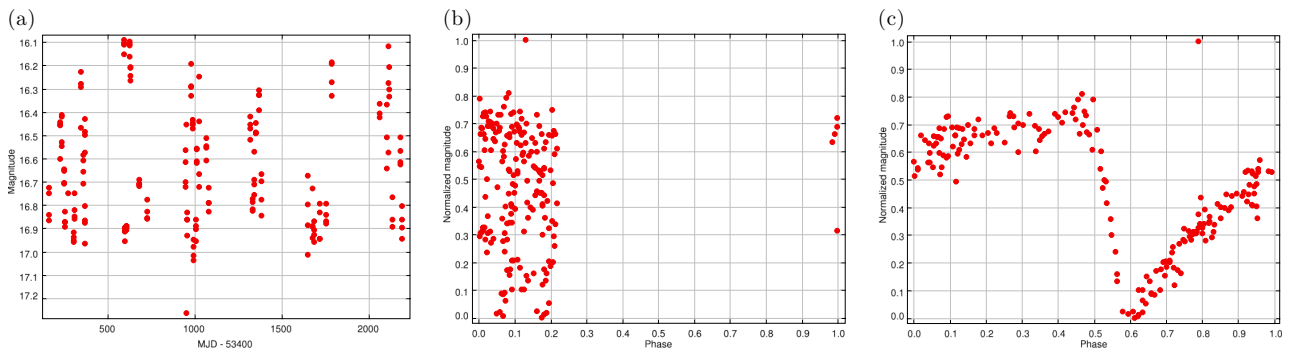
Since the definition of  $H_c$  is not dependent on the partition shape, we also consider an optimal estimator for  $H_c$  based on an optimal partitioning of the data using Bayesian blocks (BB; Scargle et al. 2012) (see Appendix A for details). We found good agreement between the values of the CE for the two partition schemes: applying the two estimators to the same data set produces conditional entropies that are strongly correlated. Differences in the numerical value are attributable to the lack of normalization in either estimator. However, the optimal partitioning scheme is computationally expensive since it involves determining the Voronoi tessellation for each trial period and this precludes it from being an efficient period-finding algorithm. We therefore adopt a simple rectangular partitioning scheme in this analysis.

Fig. 1(c) shows the light curve folded at the trial period which minimizes the CE. (See Fig. 2 for the associated periodogram – the plot of test statistic versus frequency. The search for the correct period is most commonly done using a scan through frequency space.)

The most likely periods are those associated with the strongest minima in the periodogram. Although it is possible to associate a probabilistic significance with a particular value (Cincotta et al. 1999) of this statistic, this is not a powerful enough discriminator between rare (likely) events. Rather we decided to see whether using an additional statistic to identify the correct period from the subset identified by the CE algorithm could boost the overall performance.

Thus, to assess which is the most significant of the CE minima, we calculate an AOV (Schwarzenberg-Czerny 1989) statistic for the  $k$  most likely periods and select the period which maximizes this statistic as the measured period for this time series.

We also observe that, in some cases, the CE periodogram is not flat but exhibits a weak overall dependence on frequency, i.e. there is a trend for generally lower CE values at lower frequencies. This could lead to misidentification of the strongest minima in the periodogram and so we add a normalization step of dividing the



**Figure 1.** The light curve of a typical type AB RR Lyrae from CRTS (Drake et al. 2013) (a) folded at the trial period which minimizes the entropy (b) and conditional entropy (c).

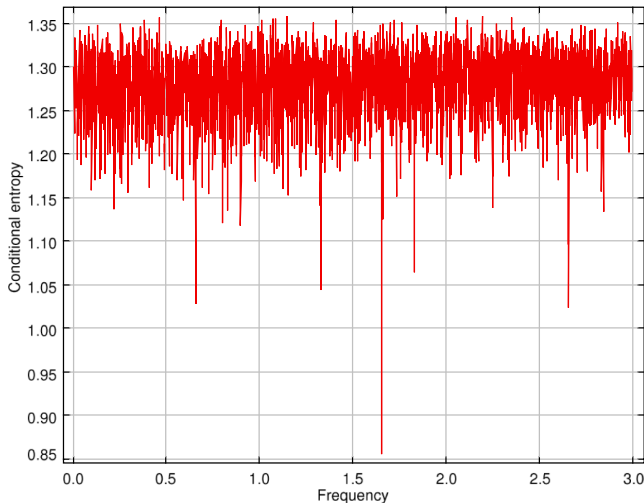


**Figure 2.** The CE periodogram (frequency in  $\text{day}^{-1}$ ) for the light curve of a typical type AB RR Lyrae from CRTS in Fig. 1. Note that there is no discernible minimum at the mean solar day period (1.002 74 d).

periodogram by a smoothed version using a wide rolling median filter before identifying the strongest minima.

Finally, we note that, as with the original Shannon entropy-based method of Cincotta et al. (1995), the algorithm does not yet explicitly take into account errors on the data. Cincotta (1999) addressed this with essentially a kernel-based estimator for the Shannon entropy and an equivalent expression is easily derivable for the CE. It is less efficient, though, as simple integer counting operations have been replaced with more complicated function calls. The effect of errors in the data are also somewhat mitigated by our use of overlapping partitions (see below) with individual data points contributing to the occupation probabilities of more than one bin as they would with a kernel.

## 2.2 Period harmonics

One particular issue for automated period finders (particularly Lomb–Scargle) is that they misidentify a multiple of the period as the ‘true’ period – this is a common problem for binary systems where the half period is frequently the most significant peak in a periodogram. For example, Richards et al. (2012) initially find 70 per cent of their periods for eclipsing binaries (EBs;  $\sim 49$  per cent of all objects) in the ASAS Catalogue of Variable Stars (ACVS; Pojmanski, Pilecki & Szczygiel 2005) to be half periods. As discussed in Wang et al. (2012), this is attributable to two aspects: for symmetric EBs, the true period and half its value are not clearly distinguishable quantitatively. Meanwhile, methods that are successful for EBs tend to find integer multiple periods of ‘single-bump’ stellar types, such as RR Lyrae and Cepheids, and vice versa.

Several techniques have been proposed to deal with this. Stellingwerf (2011) suggests ‘subharmonic averaging’ where a significant signal in the periodogram (test statistic versus frequency) is replaced by the average of the statistic value at the peak frequency (that associated with the significant statistic value) and its value at half the peak frequency. For real signals, the statistic value will be boosted whilst for false signals, the statistic value will decrease significantly. This can be computationally expensive, however, as it involves scanning through all the trial frequencies (periods) used. Wang et al. (2012) propose to include domain knowledge via a probabilistic generative filter that attempts to match light curves,

folded at both the best identified periods and their doubled values, to the learned shapes of common object types with the most likely giving the assumed value. Use of the filter gives an 18 per cent improvement in the accuracy of calculated periods against their quoted value. Richards et al. (2012) train a random forest-based supervised classifier to detect and correct for this artefact giving a 24 per cent boost to their accuracy, although they still find that 15.6 per cent of their calculated periods for all variable stars in the ACVS are actually half (14.1 per cent) or double (1.6 per cent) the true (quoted) value.

We propose a simpler approach based on fitting the light curve,  $y(\phi)$ , phased at a period,  $p$ , with a smoothing spline,  $f$ , which minimizes

$$\sum_{i=1}^n \left[ \frac{y_i - f(\phi_i)}{w_i} \right]^2 + \rho \int_{-\infty}^{\infty} (f'')^2 d\phi,$$

where  $w_i$  are the relative weights for each point and  $\rho$  is a smoothing parameter determined by a generalized cross-validation technique (Hutchinson & de Hoog 1985). Note that  $f$  is necessarily a natural cubic spline with knots at  $\phi_i$  for  $i = 1, \dots, n$ . We identify the strongest dip (minimum) in the spline and then repeat the procedure for the light curve phased at double the period, i.e.  $2p$ , and find the two strongest dips there. For an object where the measured period is the true period,  $p = p_0$ , the two dips in the  $2p$ -spline should be of the same amplitude within some measurement tolerance and also the same as the dip in the  $p$ -spline; however, for an object with  $p = p_0/2$ , i.e. most likely an eclipsing source, there should be a discernible difference between the two dips in the  $2p$ -spline, although this will not be generally true for the subclass of binaries which have equivalent minima, i.e. W UMa-type variables. We therefore consider the doubled period as the true value for objects where the difference between the two dips is greater than some threshold, the photometric error for the light curve, say, and the difference between the smaller of the two dips in  $2p$ -spline and the dip in the  $p$ -spline is also greater than a similar threshold. We note, though, that this threshold value may also be dependent on the signal-to-noise ratios (S/N) of light curves within a particular survey.

## 2.3 Data binning

Many period-finding algorithms use data binning [normally just of the phase (folded period) variable] in calculating their test statistic. The choice of binning parameters – width, number and location – can therefore have a significant effect on the resolving power of a particular method: too wide a bin leads to folded curves with similar phase distributions having the same test statistic, whilst too narrow a bin means that the test statistic is dominated by small number contributions giving a noisy representation of the phase distribution. Kovacs (1980) describes a process for the optimal phase cell number of a phase dispersion measure statistic that depends on the data length, signal form and noise level. There are also a number of more general prescriptions for selecting the optimal binning parameters when binning data – BB mentioned previously and jackknife likelihood (Hogg 2008) – or replacing the binning entirely with a suitable Bayesian prior (Loredo 2012). There is, however, no overall optimal approach amongst these.

In a sweep through a frequency (period) range, the phase distribution will vary as the trial frequency (period) varies and thus the optimal bin widths and number of bins required to cover it. However, it is computationally expensive to calculate these optimal

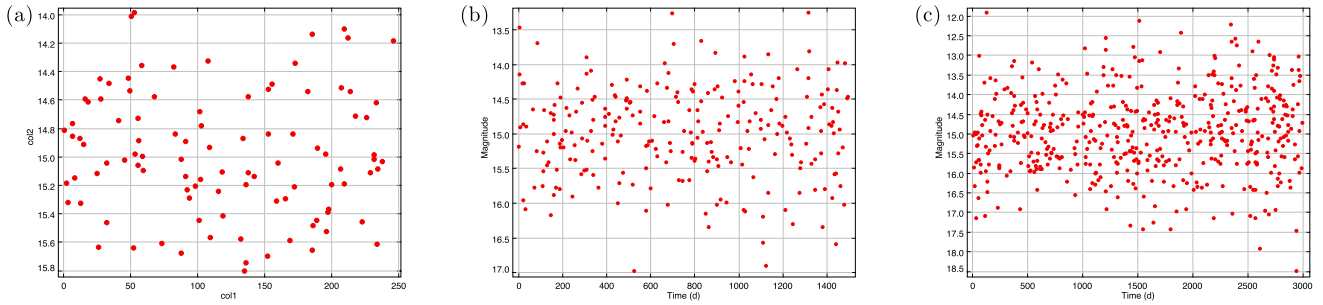


**Figure 3.** Sample synthetically generated time series for: (a) 100 points over 250 d with  $B = 0.2$  and a period of 0.752 d; (b) 250 points over 1500 d with  $B = 0.6$  and a period of 7.52 d; and (c) 500 points over 3000 d with  $B = 1.0$  and a period of 17.52 d.

values for each specific trial frequency and so fixed ‘mean’ optimal values are used in the relevant algorithms. We have determined the range of the optimal number of bins and bin widths for a set of sample light curves with numbers of observations spanning the range  $\sim 10$ –2000 using both the jackknife and BB approaches. We find that a phase bin width of  $\Delta\phi = 0.1$  (giving 10 bins) is close to optimal and use this for the algorithm; we also use a magnitude bin width of  $\Delta m = 0.2$ , determined in a similar fashion.

AOV makes use of flexible bin sizes when there is poor phase coverage and less than five points in some bins. We have adopted a similar approach for our algorithm, using an overlapping bin of width  $\Delta\phi = 0.2$  to calculate  $H_c$  and accounting for data points being included twice, e.g. a point at  $\phi = 0.25$  will be included in both the bins covering  $\phi = 0.1$ –0.3 and 0.2–0.4, respectively, when there is poor phase coverage. The PDM2 algorithm (Stellingwerf 2011) also follows a similar strategy.

We also omit all points in a light curve which are defined as outliers according to

$$\frac{|x_i - \text{med}_j x_j|}{\text{MAD}_n} > 3.0,$$

where  $\text{med}_j x_j$  is the sample median and  $\text{MAD}_n$  is the median absolute deviation from the median.

### 3 DATA SETS

In this analysis, we consider synthetic data and real data from the massive compact halo object (MACHO) surveys.

#### 3.1 Synthetic data

We generate synthetic time series with the form

$$m(t) = A_0 + \sum_{n=1}^3 A_n \sin\left(\frac{2n\pi t}{P}\right) + B\sigma,$$

where  $A_0 = 15$ ,  $A_1 = -0.5$ ,  $A_2 = 0.15$ ,  $A_3 = -0.05$ ,  $P$  is the period,  $B$  is a scaling factor ranging from 0.1 to 1.0 and  $\sigma$  is a Gaussian distributed random variable with zero mean and unit standard deviation  $[\mathcal{N}(0, 1)]$ . Periods are generated according to  $P = 10^{(p-1)}$ , where  $p$  is a random variable drawn from a lognormal distribution with zero mean and a standard deviation of 0.75 – this broadly mimics the stellar period distribution from variable surveys. We note that this form of synthetic data is fairly standard (e.g. Cincotta et al. 1995; Huijse et al. 2011), apart from the scalable noise term we are employing.

We have produced sets of 1000 light curves consisting of  $n$  points randomly spanning a temporal baseline of  $\tau$  days with noise scale

$B$  for a grid of  $(n, \tau, B)$ , such that  $n = 50$ –500 with  $\Delta n = 50$ ,  $\tau = 250$ –3000 with  $\Delta\tau = 250$  and  $B = 0.1$ –1.0 with  $\Delta B = 0.1$ . Sample light curves are shown in Fig. 3.

#### 3.2 MACHO

The MACHO survey (Alcock et al. 2003) was designed to search for gravitational microlensing events in the Magellanic Clouds and the Galactic bulge, and more than 20 million stars were observed, making it an important resource for variable star studies. A ‘gold standard’ data set of light curves has been produced from the MACHO survey by the Harvard Time Series Center, consisting of approximately 500 each of RR Lyrae, EBs and Cepheids, respectively, covering the Large Magellanic Cloud ( $75^\circ < \text{RA} < 85^\circ$ ,  $-71^\circ < \text{Dec} < -67^\circ$ ). Although MACHO data normally consist of blue and red channel data for each stellar object, only the blue channel ( $V$ -band equivalent) data have been used here. This data set has also been used in two correntropy-based (generalized correlation) approaches for estimating periods in non-uniformly sampled time series (Mishra et al. 2011; Huijse et al. 2012).

### 4 RESULTS

For each of the synthetic data sets, we have estimated the efficiency of the algorithm as a function of accuracy, i.e. the fraction of 1000 light curves with different numbers of data points, temporal coverage and noise levels the method recovers with the true period to a prescribed level of accuracy. We define our accuracy in terms of the absolute difference between the recovered period and the true period relative to the true period:

$$\text{accuracy} = \frac{|P_{\text{rec}} - P_{\text{true}}|}{P_{\text{true}}}.$$

As we noted in Section 2, a period-finding algorithm may also frequently find a period (sub)harmonic instead of the true period. To determine how close the found period is to an integer (sub)multiple of the true period, we use

$$\text{accuracy} = \left| \frac{P_{\text{rec}}}{P_{\text{true}}} - \left\| \frac{P_{\text{rec}}}{P_{\text{true}}} \right\| \right| \quad \text{for } P_{\text{rec}} > P_{\text{true}}$$

and

$$\text{accuracy} = \left| \frac{P_{\text{true}}}{P_{\text{rec}}} - \left\| \frac{P_{\text{true}}}{P_{\text{rec}}} \right\| \right| \quad \text{for } P_{\text{rec}} < P_{\text{true}},$$

where  $\|x\|$  is the nearest integer to  $x$ . As a comparison for the performance of the CE method, we have also tested the straightforward (Shannon) entropy algorithm of Cincotta et al. (1995).

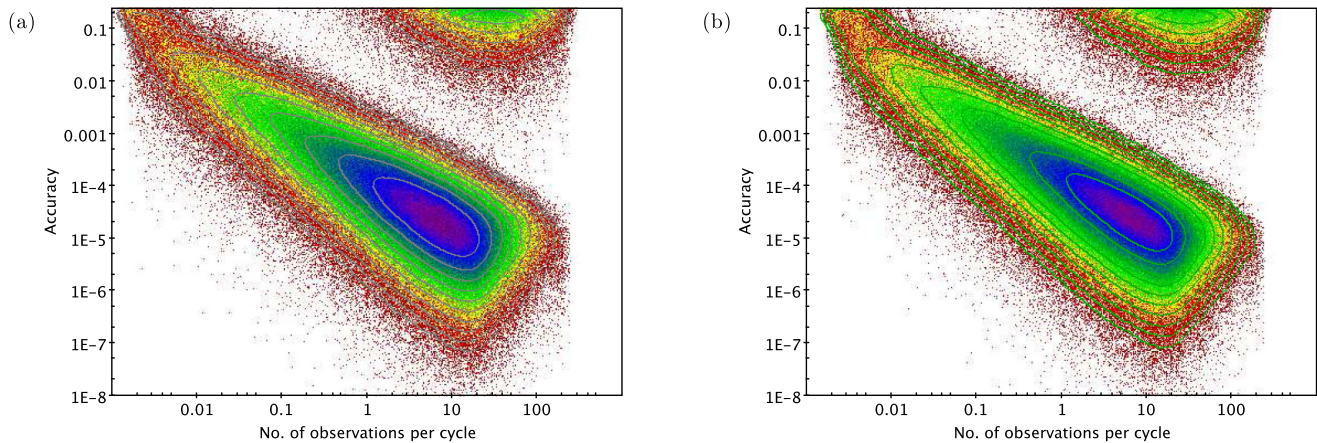


**Figure 4.** The distribution of accuracies from the synthetic data in terms of the number of observations per cycle for the two entropy-based methods: (a) CE and (b) Shannon entropy. The concentrations at poor accuracy and high observations per cycle originate with the noisiest simulated data ( $B > 0.8$ ). Both methods are successful, although the CE is marginally better – it returns slightly more objects at higher accuracies.

For each simulated light curve with a period  $P$  and  $n$  observations spanning a baseline of  $\tau$  days, we can determine the number of observations per cycle, i.e. the density of points in the folded light curve, and this allows us to easily compare the accuracies across our simulation grid, for example, that of objects with a period of 0.5 d and 50 observations over a 1 yr baseline with those with a period of 500 d and 500 observations over a 10 yr baseline.

Fig. 4 shows the distribution of accuracies against the number of observations per cycle for the two entropy-based methods with the synthetic data. Clearly, the better sampled the folded light curve, the better is the accuracy of both methods, although the CE method returns a slightly higher proportion of accurate results than the regular entropy – 5 per cent more of objects have an accuracy less than a  $10^{-5}$  cutoff with CE than with Shannon. The tracks of the median centroid of the distributions with varying  $B$  are shown in Fig. 5, indicating that as the light curves get noisier, both methods also get less accurate but that the Shannon method does so at a quicker rate – past  $B = 0.5$  there is a 0.5 dex difference in the median accuracy for the two.

Fig. 6 shows the overall accuracy distributions for the two entropy methods for the different values of the error scaling factor used. Again both methods show a dependence on how noisy the light curve is, but the CE performs slightly better in all cases, i.e. for a particular accuracy cutoff value, the CE returns a larger number of

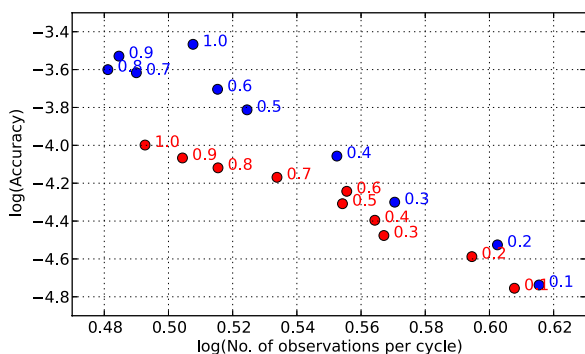


**Figure 5.** The tracks of the median centroids of the accuracy distributions from the synthetic data for the two entropy-based methods – red (CE) and blue (Shannon entropy) – with the different values of the error scaling factor,  $B$ .

periods than the Shannon entropy. This also shows the harmonic data with the CE method a much better indicator of periodicity for all noise levels. Note that for  $B > 0.7$ , most of the Shannon entropy accuracies are significantly wrong (the strong concentration in the top-right corner of Fig. 6d).

Although we have included random sampling and a noise term in our generated data, we have so far only demonstrated the efficacy of the algorithm with a synthetic sinusoidal signal which is not the most realistic situation. However, as Table 1 shows, when applied to real data with all its additional characteristics (such as observing cadences rather than random sampling and heteroscedastic errors), the CE method is vastly more effective and robust. We note that Huijse et al. (2012) get fractional recovery rates of 0.88 and 0.99 for the true period and an integer (sub)multiple of the period, respectively, for an accuracy cutoff of  $5 \times 10^{-3}$ . However, we reserve a far more extensive comparison of the CE algorithm to other period-finding techniques with real data to our companion paper (Graham et al. 2013).

The accuracy distributions for the two entropy-based methods are shown in Fig. 7. The line of CE points at  $\log(\text{accuracy}) = 0.5$  indicates those light curves (12 per cent) for which the method has incorrectly recovered a half period. As expected, these are predominantly EBs with a few type C RR Lyrae as well. A large fraction of the Shannon entropy periods (blue points) are clearly around the  $\sim 1$  d value (the phenomenon shown in Fig. 1). In fact, this is also class-related behaviour with the Shannon entropy method only correctly recovering the true periods for mainly Cepheid variables. Of the three classes in this data set, the distinguishing feature of the Cepheids is that they have a higher S/N than RR Lyrae or EBs. This makes it easier for the Shannon entropy method to identify their correctly phased light curves than the other two classes. Again we present a more extensive discussion of the class dependences of various period-finding algorithms in our companion paper.

## 5 CONCLUSIONS

In this paper, we have introduced a new period-finding algorithm based on the CE of the time series. As Cincotta (1999) suggested, this improves on the results of a basic Shannon entropy-based approach. Although CE shows similar results to existing algorithms when applied to standard synthetic data, it proves itself to be a much more powerful technique in detecting general periodicity [via an

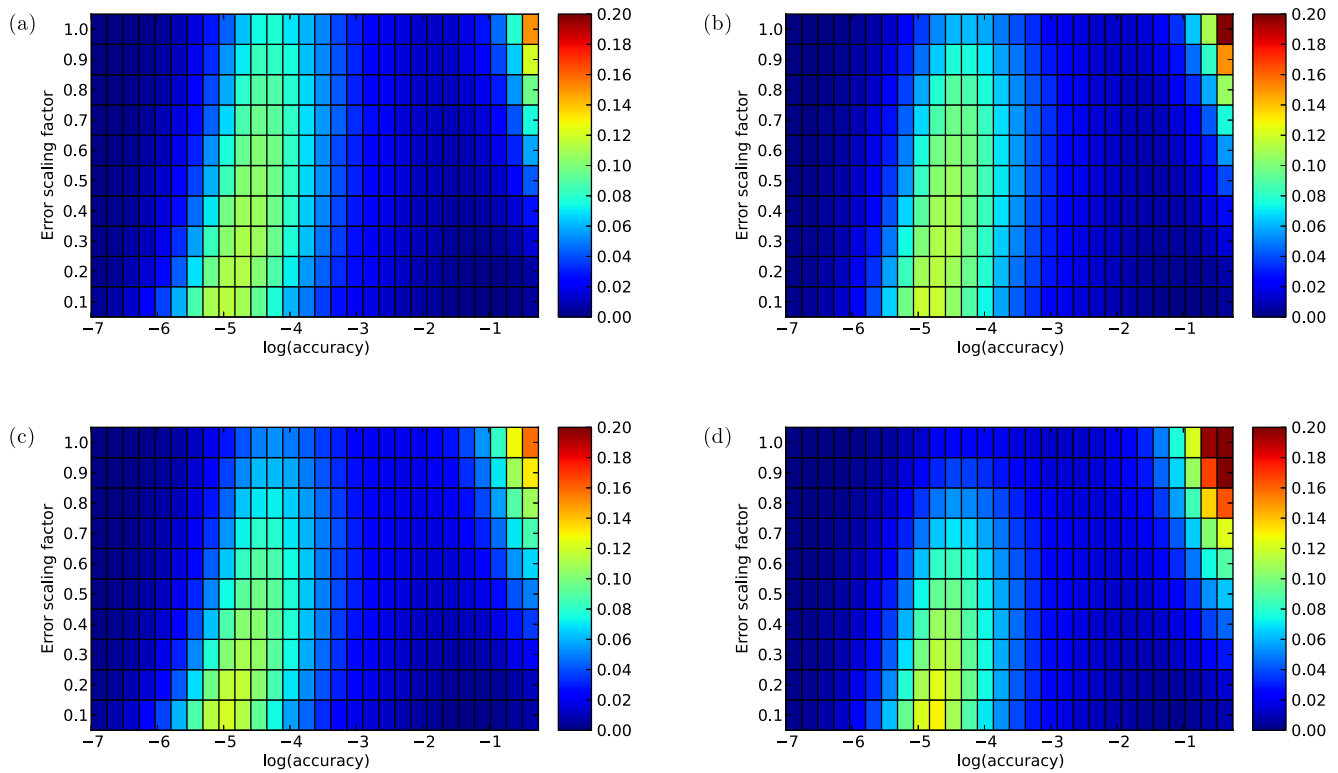


**Figure 6.** The upper plots show the normalized distribution of accuracies of the recovered period relative to the true period for the two entropy-based algorithms for the difference values of the error scaling factor,  $B$ , in the synthetic data: (a) the conditional entropy, (b) the Shannon entropy. The lower plots show the normalized distribution of accuracies of the recovered period relative to an integer (sub)multiple of the true period: (c) the conditional entropy, (d) the Shannon entropy. The conditional entropy performs moderately better at higher noise levels, particularly in detecting period harmonics.

**Table 1.** The fractional recovery rate of true periods for the two entropy algorithms with the real MACHO data and different accuracy cutoffs.

Method	True period			Harmonic		
	$10^{-5}$	$10^{-4}$	$10^{-3}$	$10^{-5}$	$10^{-4}$	$10^{-3}$
Conditional	0.47	0.82	0.86	0.52	0.94	0.99
Shannon	0.07	0.28	0.29	0.07	0.29	0.30

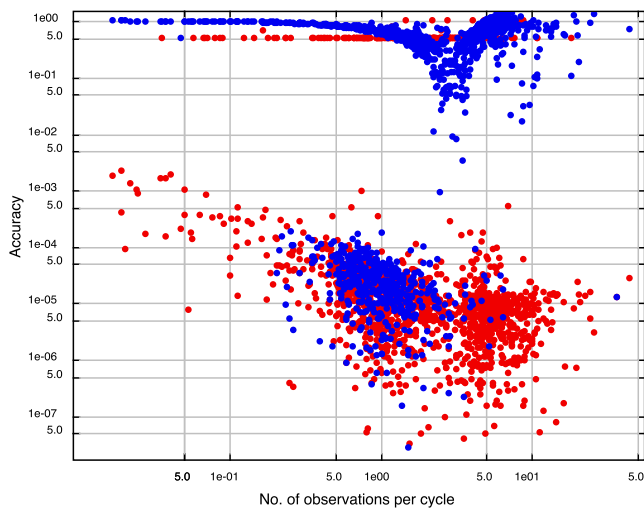


**Figure 7.** The distribution of accuracies for the MACHO data in terms of the number of observations per cycle for the two entropy-based methods: red (CE) and blue (Shannon entropy).

integer (sub)multiple of the true period] and real data. This stresses the importance of using real data whenever possible to test new techniques. Although we have only considered the application of this algorithm to single-band light curves, we think that the technique can easily be extended to multiband light curves and also to transit searches and will explore these in a future paper.

**ACKNOWLEDGEMENTS**

We thank the referee, Pablo Cincotta, for his useful comments. This work was supported in part by the NSF grants AST-0909182 and IIS-1118041, by the W. M. Keck Institute for Space Studies, and by the US Virtual Astronomical Observatory, itself supported by the NSF grant AST-0834235.

**REFERENCES**

Alcock C. et al., 2013, VizieR On-line Data Catalog: II/247  
 Baluev R. V., 2012, in Mickaelian A. M., Malkov O. Yu., Samus N. N., eds, Proc. NAS RA, Fifty Years of Cosmic Era: Real and Virtual Studies of the Sky. National Academy of Sciences of the Republic of Armenia, Yerevan, p. 230  
 Baluev R. V., 2013, MNRAS, 431, 1167  
 Cincotta P. M., 1999, MNRAS, 307, 941  
 Cincotta P. M., Mendez M., Nunez J. A., 1995, ApJ, 449, 231  
 Cincotta P. M., Helmi A., Mendez M., Nunez J. A., Vucetich H., 1999, MNRAS, 302, 582  
 de Jager O. C., Raubenheimer B. C., Swanepoel J. W. H., 1989, A&A, 221, 180  
 Drake A. J. et al., 2009, ApJ, 696, 870  
 Drake A. J. et al., 2013, ApJ, 763, 32

- Foster G., 1996, *AJ*, 112, 1709
- Graham M. J., Drake A. J., Djorgovski S. G., Mahabal A. A., Donalek C., Duan V., Maker A., 2013, *MNRAS*, in press, doi:10.1093/mnras/stt1264
- Gregory P. C., Loredo T. J., 1992, *ApJ*, 398, 146
- Hogg D., 2008, preprint (arXiv:0807.4820)
- Huijse P., Estevez P. A., Zegers P., Principe J. C., Protopapas P., 2011, *IEEE Signal Process. Lett.*, 18, 371
- Huijse P., Estevez P. A., Protopapas P., Zegers P., Principe J. C., 2012, *IEEE Trans. Signal Process.*, 60, 5135
- Hutchinson M. F., de Hoog F. R., 1985, *Numer. Math.*, 47, 99
- Ivezic Z. et al., 2011, preprint (arXiv:0805.2366)
- Kaiser N. et al., 2002, *Proc. SPIE*, 4836, 154
- Kato T., Uemura M., 2012, *PASJ*, 64, 122
- Kovacs G., 1980, *Ap&SS*, 69, 485
- Leroy B., 2012, *A&A*, 545, 50
- Lomb N. R., 1976, *Ap&SS*, 39, 447
- Loredo T., 2011, in Griffin E., Hanisch R., Seaman R., eds, *Proc. IAU Symp.* 285, *New Horizons in Time Domain Astronomy*. Cambridge Univ. Press, Cambridge, p. 87
- Miller E. G., 2003, in *International Conference on Acoustics, Speech, and Signal Processing*, Vol. 3, *A New Class of Entropy Estimators for Multi-Dimensional Densities*. IEEE, Los Alamitos, p. 297
- Mishra B. P., Principe J. C., Estevez P. A., Protopapas P., 2011, in *IEEE International Workshop on Machine Learning for Signal Processing, Estimation of Periodicity in Non-Uniformly Sampled Astronomical Data Using a 2D Kernel in Correntropy*. IEEE, Los Alamitos, p. 533
- Pojmanski G., Pilecki B., Szczygiel D., 2005, *Acta Astron.*, 55, 275
- Rau A. et al., 2009, *PASP*, 121, 1334
- Richards J. W., Starr D. L., Miller A. A., Bloom J. S., Butler N. R., Brink H., Crellin-Quick A., 2012, *ApJS*, 203, 32
- Scargle J. D., 1982, *ApJ*, 263, 835
- Scargle J. D., Norris J. P., Jackson B., Chiang J., 2012, *ApJ*, 764, 167
- Schwarzenberg-Czerny A., 1989, *MNRAS*, 241, 153
- Schwarzenberg-Czerny A., 1999, *ApJ*, 516, 315
- Stellingwerf R. F., 1978, *ApJ*, 224, 953
- Stellingwerf R. F., 2011, in McWilliam A., ed., *RR Lyrae Stars, Carnegie Observatories Astrophysics Series Vol. 5, Metal-Poor Stars, and the Galaxy*. Observatories of the Carnegie Institution of Washington, Pasadena, p. 47
- Wang Y., Khardon R., Protopapas P., 2012, *ApJ*, 756, 67
- Zechmeister M., Kurster M., 2009, *A&A*, 496, 577

## APPENDIX A: OPTIMAL ESTIMATOR FOR THE CE

Scargle et al. (2012) describe an algorithm – Bayesian blocks (BB) – that finds the optimal segmentation of 1D data in an observation interval. This can be extended to arbitrary dimensions in the following way (Scargle, private communication):

- (i) compute the 2D Voronoi tessellation of the points;
- (ii) compute the areas of the Voronoi cells;
- (iii) sort the (1D array of) areas (increasing);
- (iv) feed this array to the 1D BB algorithm;
- (v) the blocks coming out of the previous step will in general be broken up into non-connecting pieces – so at this point it may be necessary to identify these pieces – yielding a set of blocks (hyper-Voronoi regions) that are connected subsets of the Voronoi cells in the original blocks.

The (Shannon) entropy of the point distribution (light curve) can be estimated (Miller 2003) as

$$H_V = \sum_{i=1}^m \frac{C(U^i)}{N} \log \left( \frac{NA(U^i)}{C(U^i)} \right),$$

where each hyper-Voronoi region  $U^i$  has  $C(U^i)$  Voronoi regions in it,  $N = \sum_i C(U^i)$ , and  $A(U^i)$  is the 2-dimensional volume of  $U^i$ . The CE is then given by  $H(m|\phi) = H(m, \phi) - H(\phi)$ , where  $H_V = H(m, \phi)$ .  $H(\phi)$  can be estimated from the BB partitioning of the phase distribution via  $H(\phi) = -\sum_{i=1}^m f(x_i) \log(f(x_i)/w(x_i))$ , where  $f(x_i)$  is the fraction of points in the  $i$ th BB partition and  $w(x_i)$  is its width.

This paper has been typeset from a  $\text{\TeX}/\text{\LaTeX}$  file prepared by the author.